

**Supporting Information:**

**Kinetic Isotope Effects in the Water Forming  
Reaction  $\text{H}_2/\text{D}_2 + \text{OH}$  from Rigorous  
Close-Coupling Quantum Dynamics Simulations**

Ralph Welsch<sup>\*,†</sup>

*†Center for Free-Electron Laser Science, DESY, Notkestrasse 85, 22607 Hamburg,  
Germany*

*‡The Hamburg Centre for Ultrafast Imaging, Luruper Chaussee 149, 22761 Hamburg,  
Germany*

E-mail: ralph.welsch@desy.de

# Multi-configurational time-dependent Hartree approach

The calculation of the thermal flux eigenstates as well as the subsequent imaginary and real time propagation require an efficient scheme for high-dimensional wave-packet propagation. Thus, the multi-configurational time-dependent Hartree<sup>S1,S2</sup> (MCTDH) approach is employed.

The ansatz for a set of MCTDH wave functions within the state-averaged approach<sup>S3</sup> reads

$$\Psi_w(x_1, \dots, x_d, t) = \sum_{j_1=1}^{n_1} \cdots \sum_{j_d=1}^{n_d} A_{w;j_1 \dots j_d}^1(t) \prod_{k=1}^d \Phi_{j_k}^{1;k}(x_k, t). \quad (1)$$

In this two-layer representation time-dependent basis functions  $\Phi_{j_k}^{1;k}(x_k, t)$ , called single-particle functions (SPF), are used. They are subsequently expanded in a time-independent basis  $\{\chi_j^k(x_k)\}$ :

$$\Phi_{j_k}^{1;k}(x_k, t) = \sum_{i_k=1}^{N_k} A_{j_k;i_k}^{2;k}(t) \chi_{i_k}^k(x_k). \quad (2)$$

This approach can be extended to a multi-layer representation,<sup>S4,S5</sup> where the SPFs are recursively expanded in a time-dependent basis. Considering, e.g., two layers of SPFs, the multi-layer (ML) MCTDH ansatz reads

$$\begin{aligned} \Psi_w(x_1^1, \dots, x_d^1, t) &= \sum_{j_1=1}^{n_1} \cdots \sum_{j_d=1}^{n_d} A_{w;j_1 \dots j_d}^1(t) \prod_{k=1}^d \Phi_{j_k}^{1;k}(x_k^1, t), \\ \Phi_p^{1;k}(x_k^1, t) &= \Phi_p^{1;k}(x_1^{2;k}, \dots, x_{d_k}^{2;k}, t) = \sum_{j_1=1}^{n_{k,1}} \cdots \sum_{j_{d_k}=1}^{n_{k,d_k}} A_{p;j_1 \dots j_{d_k}}^{2;k}(t) \prod_{l=1}^{d_k} \Phi_{j_l}^{2;k,l}(x_l^{2;k}, t), \\ \Phi_p^{2;k,\lambda}(x_\lambda^{2;k}, t) &= \sum_{j=1}^{N_\alpha} A_{p;j}^{3;k,\lambda}(t) \chi_j^\alpha(x_\lambda^{2;k}), \\ &\text{with } \alpha = \lambda - \sum_{i=1}^{k-1} d_i. \end{aligned}$$

An efficient scheme for the propagation of MCTDH wave functions is the constant mean-field (CMF) integration.<sup>S6</sup> This work uses a revised version, the CMF2 scheme.<sup>S7</sup> Matrix elements of a general potential energy surface (PES) are obtained using the correlation DVR (CDVR)<sup>S8</sup> scheme with its multi-layer extension (ML-CDVR)<sup>S5,S9</sup> throughout this work.

## Primitive and Single-particle Basis Sets

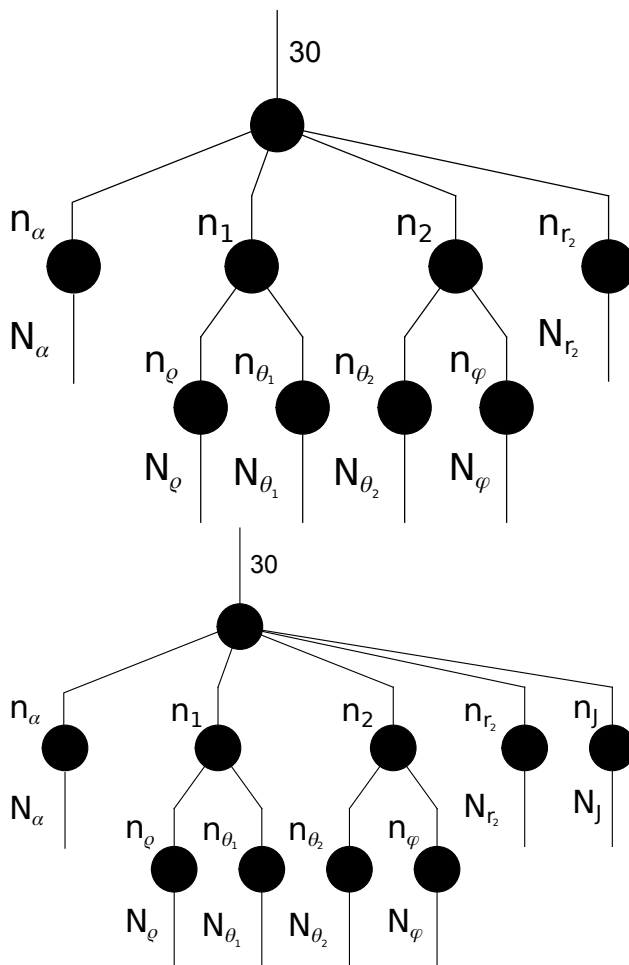


Figure S1: Structure of the ml-MCTDH wave function used. (a)  $J = 0$  simulations (b) close-coupling simulations. The basis set sizes are given in Tabs. S1 to S6.

The primitive basis sets employed are given in Tabs. S1 and S2. The structure of the multi-layer MCTDH wave function is shown in Fig. S1. The time-dependent basis set sizes employed in the thermal flux eigenstate calculation are given in Tabs. S3 and S5 and for the

imaginary and real time propagations in Tabs. S4 and S6 for the  $J = 0$  and close-coupling simulations, respectively.

**Table S1: The time-independent grids used for  $J = 0$  simulations. See also Fig. S1.**

Coordinate	Grid type	Grid size	range
$\rho$	128	FFT	130 - 550 a.u.
$\alpha$	128	FFT	0.15 - 2.0 a.u.
$\theta_1$	96	Legendre-DVR	
$\theta_2$	64	Legendre-DVR	
$\varphi$	64	FFT	0 - $2\pi$
$r_1$	15	Hermite-DVR	

**Table S2: The time-independent grids used for close-coupling simulations. See also Fig. S1.**

Coordinate	Grid type	Grid size	range
$\rho$	256	FFT	130 - 550 a.u.
$\alpha$	256	FFT	0.15 - 2.0 a.u.
$\theta_1$	128	Legendre-DVR	
$\theta_2$	64	Legendre-DVR	
$\varphi$	64	FFT	0 - $2\pi$
$r_1$	15	Hermite-DVR	

**Table S3:** The number of SPFs used in the flux eigenstate calculations employing  $J = 0..$  See also Fig. S1.

	<b>s</b>
$n_\alpha$	7
$n_1$	28
$n_2$	28
$n_\rho$	7
$n_{\theta_1}$	7
$n_{\theta_2}$	7
$n_\varphi$	7
$n_{r_2}$	1

**Table S4:** The number of SPFs used in the imaginary and real time propagations employing  $J = 0$ . See also Fig. S1.

	<b>s</b>	<b>m</b>	<b>B</b>	<b><math>\Gamma</math></b>
$n_\alpha$	7	9	11	18
$n_1$	28	36	45	54
$n_2$	28	36	45	54
$n_\rho$	7	9	10	12
$n_{\theta_1}$	7	9	10	12
$n_{\theta_2}$	7	9	10	11
$n_\varphi$	7	9	10	12
$n_{r_2}$	1	1	1	1

**Table S5:** The number of SPFs used in the flux eigenstate calculations for close-coupling. See also Fig. S1.

	<b>s</b>	<b>m1</b>	<b>m2</b>
$n_\alpha$	5	7	7
$n_1$	15	17	17
$n_2$	15	21	21
$n_\rho$	5	6	6
$n_{\theta_1}$	5	6	6
$n_{\theta_2}$	5	6	6
$n_\varphi$	5	8	8
$n_{r_2}$	1	1	1
$n_J$	3	5	7

**Table S6: The number of SPFs used in the imaginary and real time propagations for close-coupling. See also Fig. S1.**

	<b>s</b>	<b>m1</b>	<b>m2</b>	<b>B1</b>	<b>B2</b>	$\Gamma_1$	$\Gamma_2$
$n_\alpha$	5	7	7	11	11	13	13
$n_1$	15	17	17	28	28	36	36
$n_2$	15	21	21	28	28	36	36
$n_\rho$	5	6	6	8	8	9	9
$n_{\theta_1}$	5	6	6	9	9	10	10
$n_{\theta_2}$	5	6	6	7	7	8	8
$n_\varphi$	5	8	8	10	10	12	12
$n_{r_2}$	1	1	1	1	1	1	1
$n_J$	3	5	7	5	7	5	7

## Convergence Tests for $J = 0$

The convergence of the thermal rate constants employing J-shifting with respect to SPF basis sets and the reference temperature are given in Figs. S3 and S2, respectively. For a definition of the basis sets see Tab. S4. For higher reference temperature, deviations of over an order of magnitude at the lowest temperatures considered are observed. The results obtained with reference temperatures of 400K or 300K give converged results even down to the calculation of thermal rate constants at 150K. For these two reference temperatures, very good basis set convergence is found. The error in the thermal rate constant at 150 K is estimated to be less than 10 %.

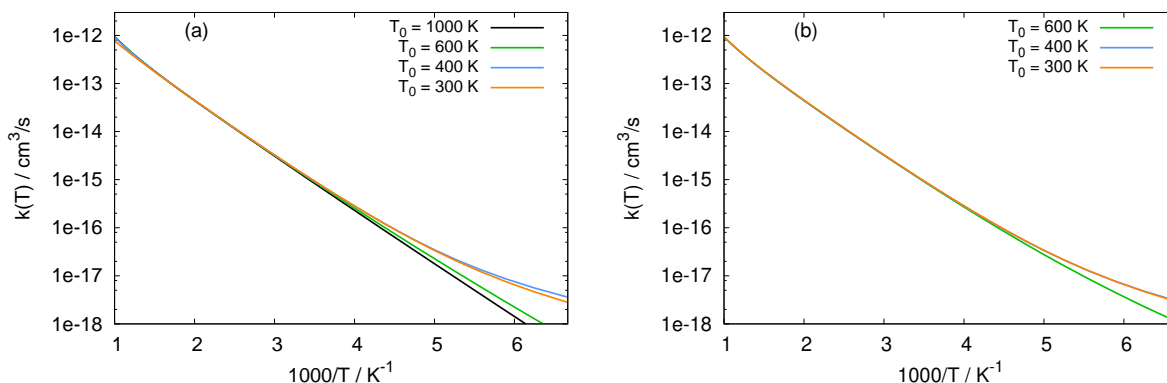


Figure S2: Thermal rate constants obtained through J-shifting for different reference temperatures  $T_0$  and basis set sizes (see Tab. S4). (a) **B** basis (b)  $\Gamma$  basis.

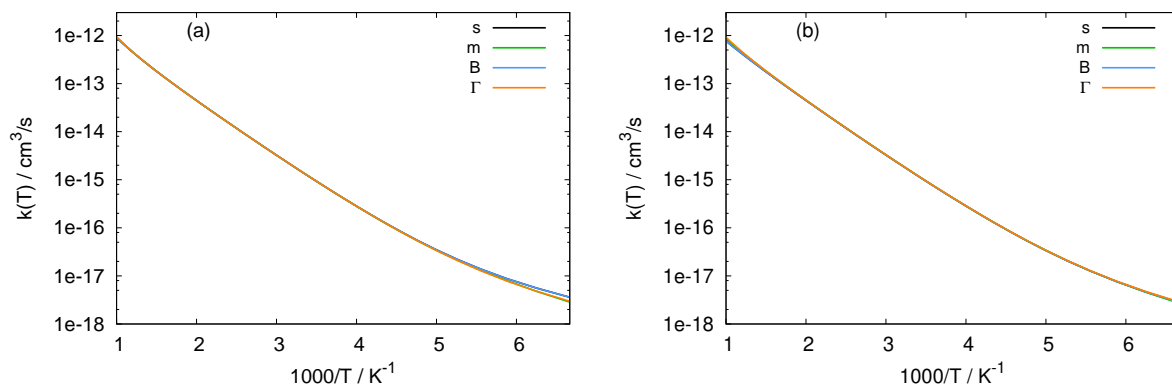


Figure S3: Thermal rate constants obtained through J-shifting for different basis set sizes (see Tab. S4) and reference temperatures  $T_0$ . (a)  $T_0 = 400$  K. (b)  $T_0 = 300$  K.

# Convergence Tests for Close-Coupling

The convergence of the thermal rate constants with respect to SPF basis sets and the reference temperature for close-coupling simulations are given in Figs. S4 and S5, respectively. For a definition of the basis sets see Tab. S6. Convergence of thermal rate constants employing close-coupling calculations are more demanding and least the basis set **B** is needed for convergence at low reference temperatures. At the lowest reference temperature employed, good convergence is achieved and the rates at 250 K differ by less than 10 % for the four largest basis sets employed. With respect to the reference temperature, it can be seen that the higher reference temperatures give larger errors for rates below 300K.

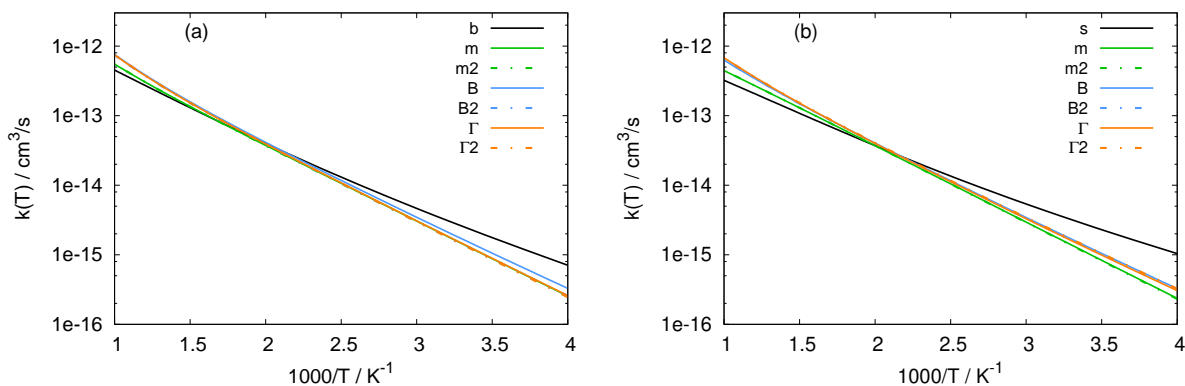


Figure S4: Close-coupling thermal rate constants for different basis set sizes (see Tab. S6) and reference temperatures  $T_0$ . (a)  $T_0 = 750$  K. (b)  $T_0 = 600$  K.

## References

- (S1) Meyer, H.-D.; Manthe, U.; Cederbaum, L. S. The Multi-Configurational Time-Dependent Hartree Approach. *Chem. Phys. Lett.* **1990**, *165*, 73–78.
- (S2) Manthe, U.; Meyer, H.-D.; Cederbaum, L. S. Wave-Packet Dynamics within the Multi-configuration Hartree Framework: General Aspects and Application to NOCl. *J. Chem. Phys.* **1992**, *97*, 3199–3213.

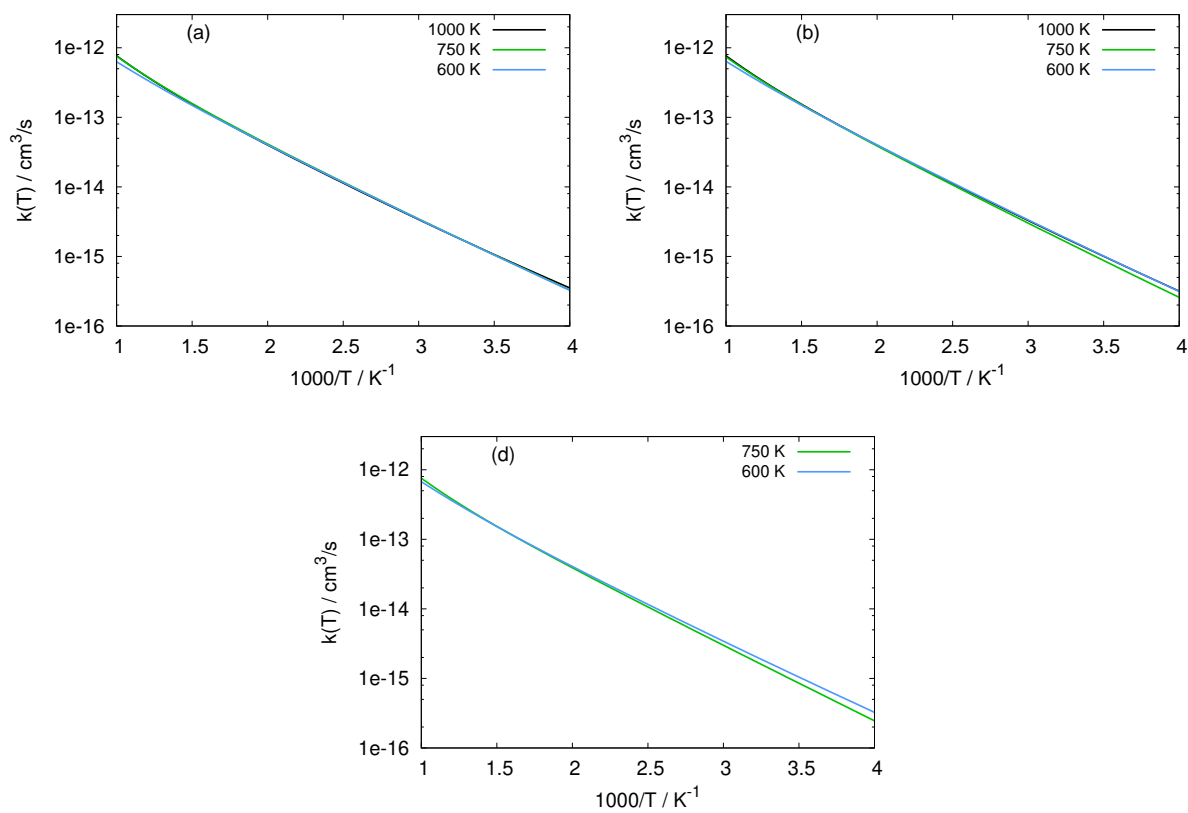


Figure S5: Close-coupling thermal rate constants for different reference temperatures  $T_0$  and different basis set sizes (see Tab. S6). (a) **B** basis (b) **B2** basis (c)  $\Gamma$  basis (d)  $\Gamma2$  basis.

- (S3) Manthe, U. The State Averaged Multiconfigurational Time-Dependent Hartree Approach: Vibrational State and Reaction Rate Calculations. *J. Chem. Phys.* **2008**, *128*, 064108.
- (S4) Wang, H.; Thoss, M. Multilayer Formulation of the Multiconfiguration Time-Dependent Hartree Theory. *J. Chem. Phys.* **2003**, *119*, 1289–1299.
- (S5) Manthe, U. A Multilayer Multiconfigurational Time-Dependent Hartree Approach for Quantum Dynamics on General Potential Energy Surfaces. *J. Chem. Phys.* **2008**, *128*, 164116.
- (S6) Beck, M. H.; Meyer, H.-D. An Efficient and Robust Integration Scheme for the Equations of Motion of the Multiconfiguration Time-Dependent Hartree (MCTDH) Method. *Z. Phys. D* **1997**, *42*, 113–129.
- (S7) Manthe, U. On the Integration of the Multi-Configurational Time-Dependent Hartree (MCTDH) Equations of Motion. *Chem. Phys.* **2006**, *329*, 168–178.
- (S8) Manthe, U. A Time-Dependent Discrete Variable Representation for (Multiconfiguration) Hartree Methods. *J. Chem. Phys.* **1996**, *105*, 6989–6994.
- (S9) Manthe, U. Layered Discrete Variable Representations and Their Application within the Multiconfigurational Time-Dependent Hartree Approach. *J. Chem. Phys.* **2009**, *130*, 054109.